Registration No.
29849

-Technical Report-

Evinrude 30 MFE Outboard, Test Configuration Torsional Vibration Analysis

Andrew L. Wiegand

U.S. Army Tank Automotive Research,
Development, and Engineering Center
Detroit Arsenal
Warren, Michigan 48397-5000

REPORT DOCUMENTATION PAGE

Form Approved
OMB No. 0704-0188

1. REPORT DATE *(DD-MM-YYYY)*	**2. REPORT TYPE**	**3. DATES COVERED** *(From - To)*
12-05-2017	Technical Report	12-05-2017

4. TITLE AND SUBTITLE

Evinrude 30 MFE Outboard, Test Configuration Torsional Vibration Analysis

5a. CONTRACT NUMBER
N/A

5b. GRANT NUMBER
N/A

5c. PROGRAM ELEMENT NUMBER
N/A

6. AUTHOR(S)

Andrew L. Wiegand

5d. PROJECT NUMBER
N/A

5e. TASK NUMBER
N/A

5f. WORK UNIT NUMBER
N/A

7. PERFORMING ORGANIZATION NAME(S) AND ADDRESS(ES)

U.S. Army Tank Automotive Research Engineering Development Center (TARDEC)
Ground Vehicle Power and Mobility (RDTA-RTI-GVPM)
6501 E. 11 Mile Rd.
Warren, MI 48397

8. PERFORMING ORGANIZATION REPORT NUMBER

TARDEC 29849

9. SPONSORING / MONITORING AGENCY NAME(S) AND ADDRESS(ES)

U.S. Army Tank Automotive Research Engineering Development Center (TARDEC)
Ground Vehicle Power and Mobility (RDTA-RTI-GVPM)
6501 E. 11 Mile Rd.
Warren, MI 48397

10. SPONSOR/MONITOR'S ACRONYM(S)

N/A

11. SPONSOR/MONITOR'S REPORT NUMBER(S)

N/A

12. DISTRIBUTION / AVAILABILITY STATEMENT

UNCLASSIFIED: Distribution Statement A. Approved for public release; distribution is unlimited.

13. SUPPLEMENTARY NOTES

None.

14. ABSTRACT

A collaborative effort was undertaken between Keweenaw Research Center at Michigan Technological University (MTU) and US Army Tank, Automotive, Research, Development and Engineering Center (TARDEC), Ground Vehicle Power and Mobility (GVPM) to evaluate the performance of an Evinrude 30 MFE outboard engine for watercraft. To support design of this test setup, and also to provide information into an assessment of the Evinrude 30 MFE's applicability to Army ground applications, a torsional vibration analysis (TVA) was completed at GVPM. The linearized eigenvalue solution of the Evinrude 30 MFE torsional vibration model indicates that the first resonant frequency will be present at approximately 29 Hz. This mode shape is characterized as the powerhead inertia being out of phase with the lower unit and dynamometer, which correlates with industry input suggesting that the lower unit of small outboards tends to fail when coupled to a dynamometer. As originally designed, engine speeds of approximately 750 to 1050 RPM (25-35 Hz) will most likely rapidly accumulate damage to the lower unit in this test configuration.

15. SUBJECT TERMS

Bradley, coupler, spring coupler, ECP2, M2A3, M7A3, torsional vibration

16. SECURITY CLASSIFICATION OF:			**17. LIMITATION OF ABSTRACT**	**18. NUMBER OF PAGES**	**19a. NAME OF RESPONSIBLE PERSON**
					Andrew Wiegand
a. REPORT	**b. ABSTRACT**	**c. THIS PAGE**		23	**19b. TELEPHONE NUMBER** *(include area code)*
UNCLASSIFIED	UNCLASSIFIED	UNCLASSIFIED			586-282-1770

Evinrude 30 MFE Outboard, Test Configuration Torsional Vibration Analysis

2017-12-05

Prepared by:

Andrew Wiegand
Mechanical Engineer
andrew.l.wiegand.civ@mail.mil
Non-Primary Power Systems
Ground Vehicle Power and Mobility (GVPM)
Tank Automotive Research Development Engineering Center (TARDEC)

Contents

Figures

1. Executive Summary

The Keweenaw Research Center at Michigan Technological University (MTU) was awarded W56HZV-14-C-0286, Work Directive 13 (WD13) by US Army Tank, Automotive, Research, Development and Engineering Center (TARDEC), Ground Vehicle Power and Mobility (GVPM). Part of this WD's objective was to develop a "Small Engine Technology Roadmap" and examine applicable technologies that would help guide TARDEC's efforts into expeditionary power sources based on combustion engine technologies. One of the engine technologies of interest was conversions of direct-injected gasoline engines from the power sports and marine industries to heavy fuels, such as NATO STANAG 3737 F-24 (Jet A fuel with additive package) and ASTM D975 ULSD2 (ultra-low sulfur diesel fuel #2).

In support of this research, GVPM engineers were able obtain three Evinrude 30 MFE outboard motors, intended for light watercraft, from Program Manager Sets, Kits, Outfits and Tools (PM SKOT) for MTU to test. MTU co-principal investigator Dr. Scott Miers and mechanical engineering researcher Dr. Brian Eggart from the Mechanical Engineer department leveraged their industry contacts to develop a best-practice test setup for these outboard motors. To support design of this test setup, and also to provide information into an assessment of the Evinrude 30 MFE's applicability to Army ground applications, a torsional vibration analysis (TVA) was completed by Andrew Wiegand at TARDEC GVPM.

The linearized eigenvalue solution of the Evinrude 30 MFE torsional vibration model indicates that the first resonant frequency will be present at approximately 29 Hz. This mode shape is characterized as the powerhead inertia being out of phase with the lower unit and dynamometer, which correlates with industry input suggesting that the lower unit of small outboards tends to fail when coupled to a dynamometer. As originally designed, engine speeds of approximately 750 to 1050 RPM (25-35 Hz) will most likely rapidly accumulate damage to the lower unit in this test configuration. A sensitivity analysis suggests that this mode shape can be shifted out of the engine operating range by increasing the dynamometer inertia to 0.057 kg-m^2 or greater.

2. Torsional Vibration Analysis Methodology

Three steps were taken to create the torsional vibration model for this test setup. First, an Evinrude 30 MFE was disassembled, inspected, and the inertias/stiffness of the system were "grouped." Second, the inertia and stiffness values were calculated and converted to energy-equivalent values. Finally, the model was assembled in Siemens LMS Imagine.Lab AMESim and a linear-analysis model was completed.

This model was developed based on personal experience and best judgment regarding the level of fidelity required to obtain the lowest frequency mode shapes. It should only be considered an estimation and needs further refinement before attempting to predict torsional vibration amplitudes. Personal experience suggests that the modes predicted will be within ±10% of the actual resonance frequency. The simplification process shown here often results to an overestimation of mode frequency as a result of numerical stiffness.

2.1 Inspection and Inertia Grouping

The Evinrude 30 MFE outboard engine consists of a 2 cylinder, 2 stroke engine coupled to a gearbox that spins a propeller. In the test configuration, this propeller will be removed and replaced with a driveshaft and rubber coupling (Mercury PN 76850A2) connected to a Froude-Hoffeman EC26TC Engine Dynamometer. A schematic of this system and the final equivalent inertia/stiffness torsional vibration model can be found in Figure 1.

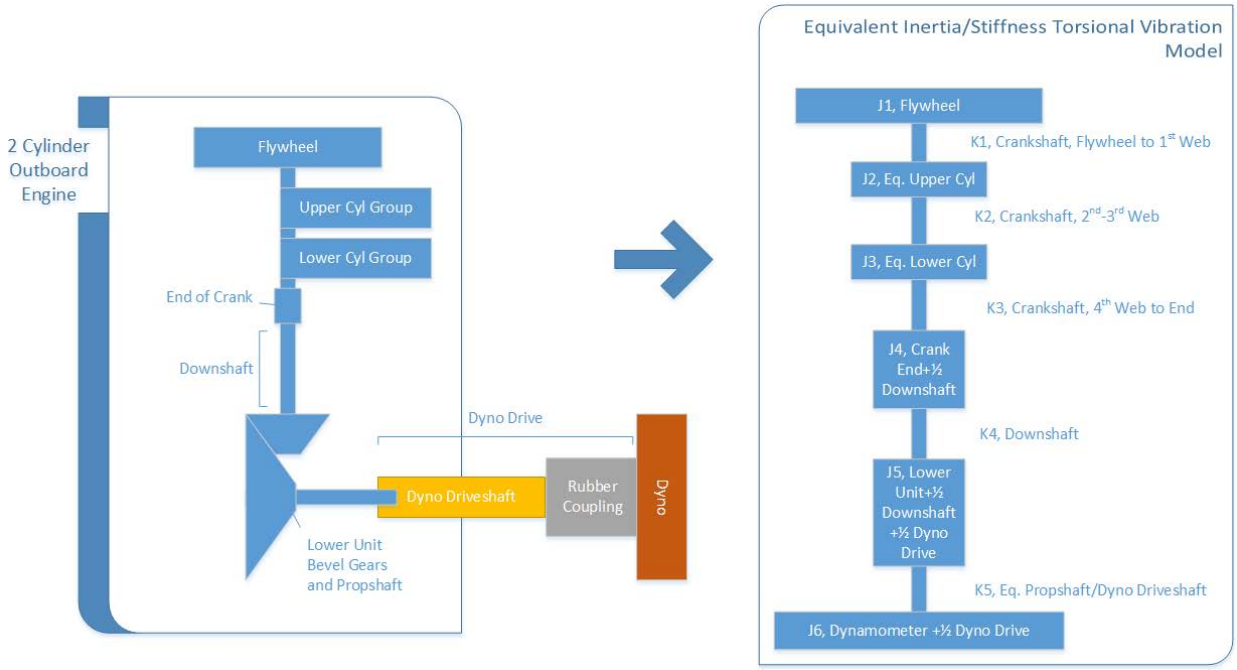

Figure 1: Engine and Test Setup Schematic and Equivalent Inertia/Stiffness Torsional Vibration Model

For reference purposes, the following nomenclature is commonly applied to marine outboard engines. The engine assembly is called the "powerhead." The gearbox that acts as a speed reducer is called the "lower unit." The shaft that connects the lower unit to the propeller is called the "propshaft."

The inertia of the powerhead was grouped after disassembly and inspection. The flywheel is located opposite the engine power take off and connected via a keyway to the crankshaft, which was assumed

to be infinitely rigid. There are no rotating ancillaries off the flywheel or the engine, so the flywheel was taken as a discrete inertial body (Figure 1, J1). Next, a common practice for developing engine models is to linearize and approximate inertia by each "cylinder line." This linearization includes approximating a constant "reciprocating" inertia created by the piston assembly through its sinusoidal motion and adding that value to the constant inertia created by each "throw" of the crankshaft. Each cylinder was given its own discrete inertial body (Figure 1, J2 and J3). Finally, the Evinrude has a section of crankshaft below the lower cylinder which mates to a long "downshaft" that connects the engine and lower unit. The inertia of this crankshaft section and half of the downshaft inertia was given its own inertial body in the model (Figure 1, J4).

The next grouping was the lower unit and dynamometer connections. The primary focus of this model was rigid-body mode shapes, and consequently gear mesh stiffness was assumed to be infinite. With this assumption, the inertia of the lower unit was grouped as a single inertia value (Figure 1, J5) including half of the shaft connecting the lower unit and powerhead, pinion, gear, propshaft and half of the approximated value of the dynamometer driveshaft.

The final grouping was of the dynamometer system. For this section, all connections (spline or bolted) were assumed to be infinitely rigid. This means the dyno, coupling, and half of the dynamometer driveshaft were lumped into a single inertial body (Figure 1, J6).

After segmenting the system into a series of inertias, torsional stiffness segments were identified. In the powerhead, stiffnesses were taken as shown in Figure 2. K1 was taken from the mating of the flywheel and crankshaft up to the first crank counterweight, K2 was taken from the second to third counterweight, and K3 was taken from the fourth counterweight to approximately half of the spline engagement length. The connections between counterweights were assumed to be infinitely rigid. K4 was taken as the torsional stiffness of the downshaft, which is a 0.624" diameter shaft with splined ends that were assumed rigid. K5 was approximated as the equivalent of three stiffnesses. These included the propshaft from the lower unit gear to half of the prop splines, an estimate of the to-be-designed driveshaft, and the rubber coupler.

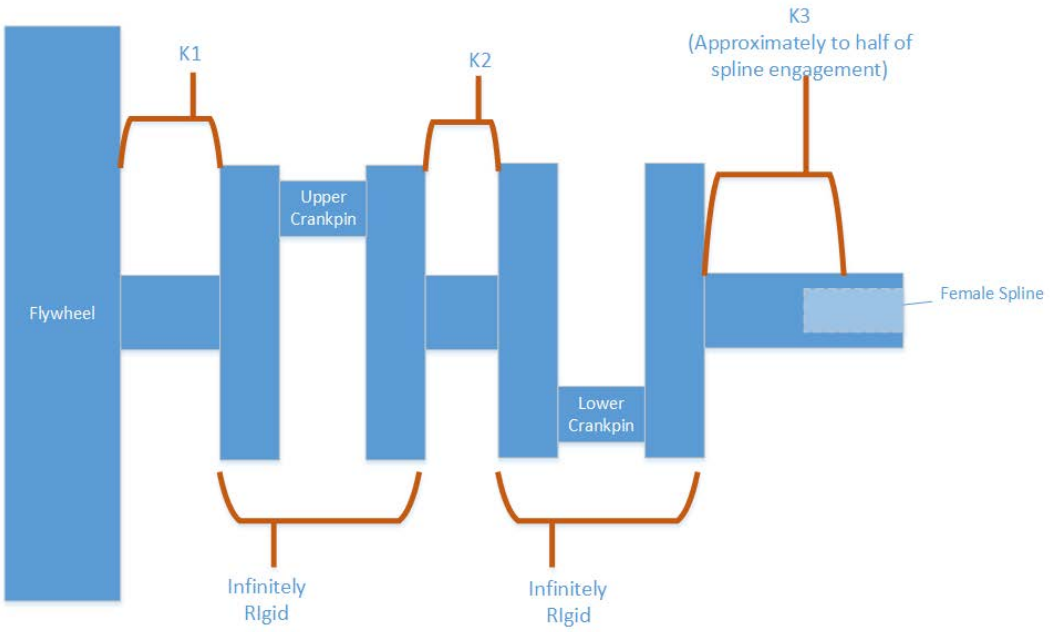

Figure 2: Stiffness Segments Assumed on 2 Cylinder Crankshaft

2.2 Parameter Estimation

Values for the inertia and stiffnesses identified were collected through a variety of means, including modeling and analysis in PTC Creo 3, engineering estimation based on similar components, and physical measurements.

For all stiffness estimations, the Creo 3 Analysis tool was used to apply a 100 Nm torque while holding the opposite location fixed. The displacement at the loaded radius was then measured and torsional stiffness was computed according to Equation 1. This equation assumes that the simulated linear displacement is small enough to be considered orthogonal to the radius.

Equation 1: Stiffness Calculation for Creo Analyses

$$K\left(\frac{Nm}{rad}\right) = \frac{100\ Nm}{\arctan\left(\frac{displacement}{radius}\right)}$$

2.2.1 J1, Flywheel

The flywheel inertia was estimated by modeling the disassembled flywheel in PTC Creo 3. The model was assigned the density of steel and was found to be approximately 0.5 pound heavier than the physical flywheel. The inertia analysis can be seen in Figure 3 and produced a value of 33650.5 kg-mm^2.

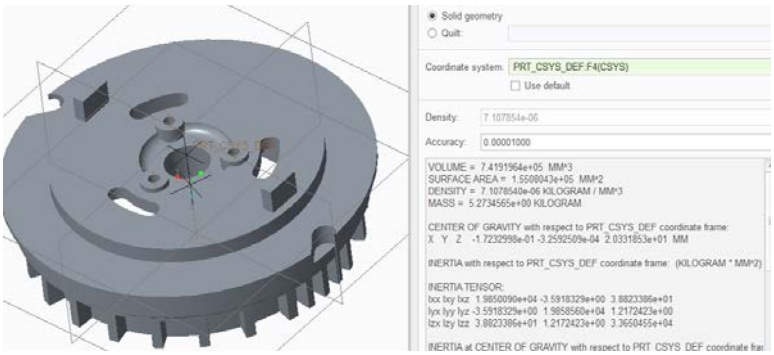

Figure 3: Inertia Measurement of Flywheel Model

2.2.2 J2, Equivalent Upper Cylinder Line

The equivalent upper cylinder line inertia was estimated using Equation 3, Equation 4 and the Creo 3 inertia measurement of a portion of the crankshaft. These equations were taken from A Handbook on Torsional Vibration, by E.J. Nestorides and published in 1958 by Cambridge Press. There derivations can be found there.

Equation 2: Approximate Inertia of a "Cylinder Group"

$$J_{CylEq} = J_{CS} + J_{rot} + \mathrm{J_{recip}}$$

$Where$:

$J_{CylEq} = \ Approximate\ inertia\ of\ a$ cylinder group

$J_{CS} = Inertia\ of\ a\ crank\ segment, determined\ subjectively$

$J_{recip} = Approximated\ inertia\ of\ reciprocating\ components$

$J_{rot} = Approximated\ inertia\ of\ rotating\ components$

Equation 3: Approximate Inertia of the Rotating Portion of Power Cylinder Components

$$J_{rot} = M_{rot} * S^2$$

$Where$:

$J_{rot} = Approximated\ inertia\ of\ rotating\ components\ (kg - mm^2)$

$M_{rot} = Approximate\ mass\ of\ the\ rotating\ portion\ of\ the\ connecting\ rod\ (kg)$

$S = Stroke\ of\ piston\ (mm)$

Equation 4: Approximate Inertia of the Reciprocating Portion of Power Cylinder Components

$$J_{recip} = \frac{1}{2} * \left(M_{CR,Recip} + M_{PA}\right) * S^2$$

$Where$:

$J_{recip} = \ Equivalent\ inertia\ of\ reciprocating\ components\ (kg - mm^2)$

$M_{CR,Recip} = Approximate\ mass\ of\ the\ reciprocating\ portion\ of\ the\ connecting\ rod\ (kg)$

$M_{PA} = Mass\ of\ the\ piston\ assembly, including\ piston, rings, wrist\ pin, and\ bearing\ (kg)$

$S = Stroke\ of\ piston\ (mm)$

J_{CS} was estimated by modeling the crankshaft in Creo 3 and completing an inertia analysis using the material properties of steel. This analysis can be seen in Figure 4 and produced an inertia value of 2246.1 kg-mm^2.

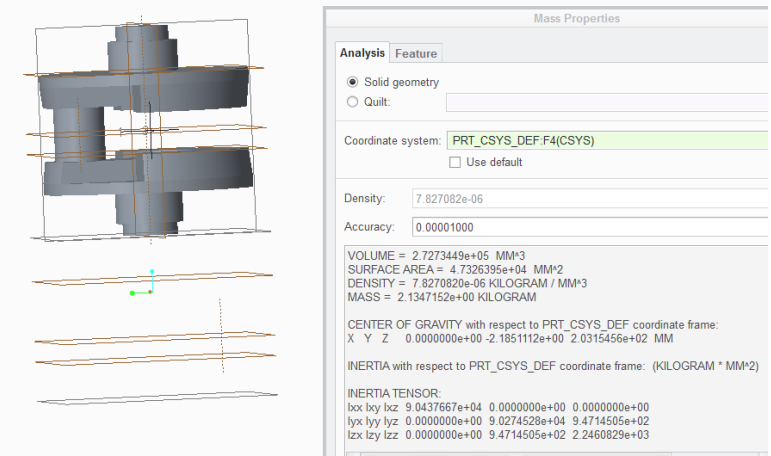

Figure 4: Inertia Measurement of J_{CS} for the Upper Cylinder

J_{rot} could not be readily estimated without further engine disassembly and was assumed to be negligible compared to the crank counterweights and reciprocating inertia. Inclusion of this inertia would be a good improvement at a later date, however.

J_{recip} was found by estimating the mass of ½ the connecting rod, measuring the mass of the piston assembly, and using the published stroke. Half the connecting rod was estimated at 83 g by placing the piston end of the connecting rod on a scale and leveling the connecting rod. The piston, rings, piston pin, retaining clips, and needle bearing were removed and found to have mass of 460 g. The published stroke is 63.5 mm. Using Equation 4, the estimated reciprocating inertia is 1094.8 kg-mm^2.

2.2.3 J3, Equivalent Lower Cylinder Line

The process used to find J2 was repeated for J3. Figure 5 shows the Creo inertia measurement with a value of 2227 kg-mm^2. This provides an equivalent inertia for the cylinder line of 3322 kg-mm^2.

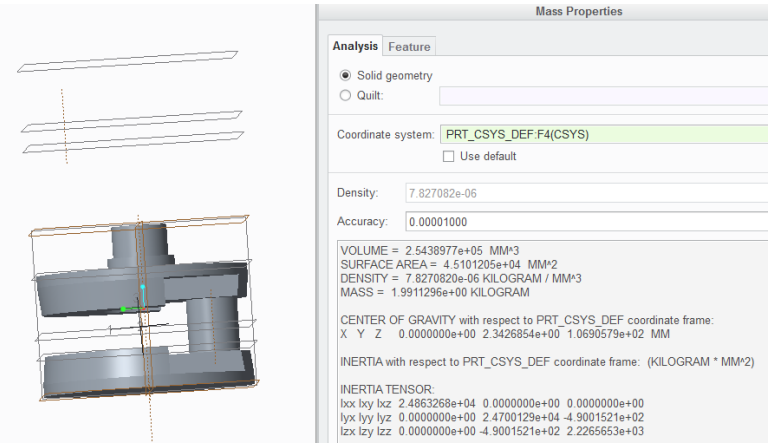

Figure 5: Inertia Measurement of J_{CS} for the Lower Cylinder

2.2.4 J4, Crankshaft End + ½ Downshaft

The inertia of J4 was taken from Creo 3 inertia measurements. The crankshaft end inertia was added to half of the downshaft inertia. Splitting the downshaft inertia is an approximation to create point inertias

instead of the true inertia distribution over the length of the shaft. These values are 47.7 and 16.7 kg-m^2.

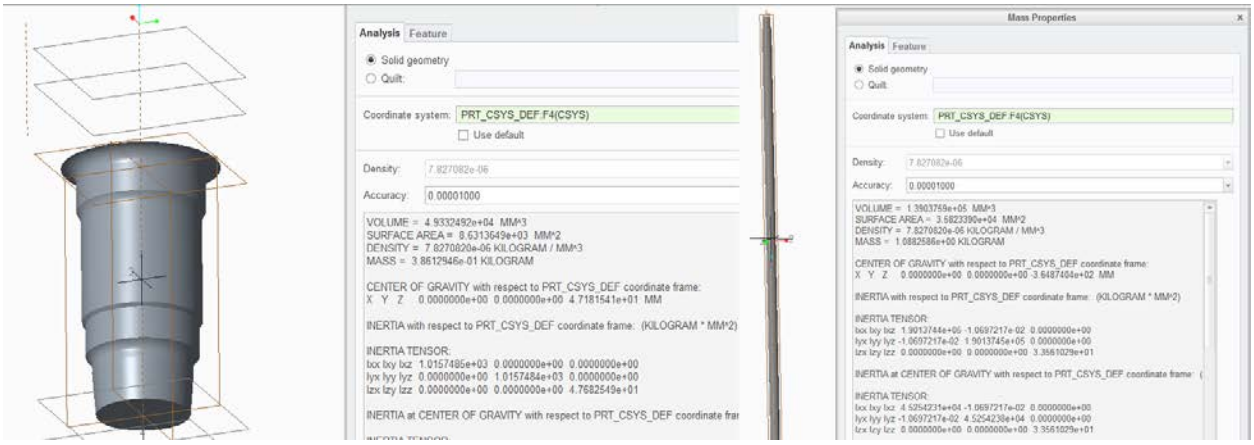

Figure 6: Inertia Measurement of Crankshaft End and Downshaft

2.2.5 J5, Lower Unit + ½ Downshaft + ½ Dyno Drive

J5 was estimated through Creo 3 inertia measurement and two engineering estimates. This value may be more inaccurate than typical because the lower unit was not disassembled in effort to preserve the assembly. All measurements were made based on observations from the technical manuals and outer measurements of the lower unit. Figure 7 shows the approximate model of the lower unit gear and propshaft through half of the splined length. The lower unit pinion was taken to be 1/2.15 times (the lower unit speed ratio) the gear inertia, or 136.5 kg-mm^2. The dyno drive was estimated to be 40 kg-mm^2 total.

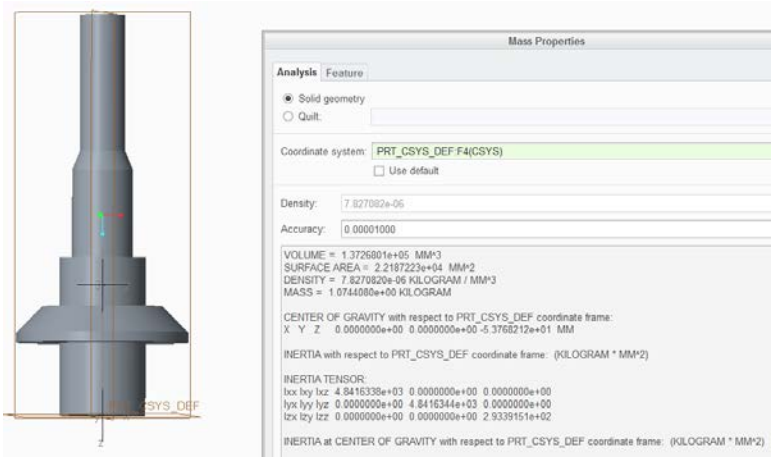

Figure 7: Inertia Measurement of Lower Unit Gear and Propshaft

2.2.6 J6, Dynamometer + ½ Dyno Drive

The dynamometer inertia was provided by Dr. Scott Miers as 31000 kg-mm^2. 20 kg-mm^2 was added to account for the dyno drive. The rubber coupler was estimated to have an inertia of 1000 kg-mm^2.

2.2.7 K1, Crankshaft, Flywheel to First Web

K1 was estimated using the Creo 3 Analysis tools. The results are shown in Figure 8. Using Equation 1 and a radius of 49.5 mm, this result suggests a stiffness of 185,185 Nm/rad.

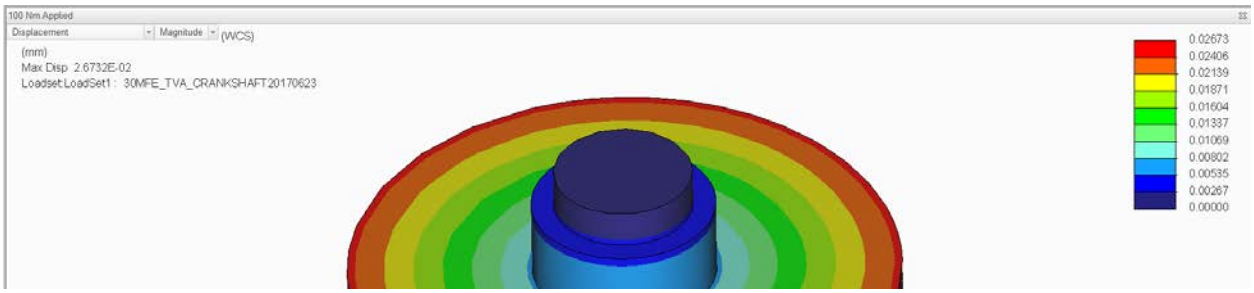

Figure 8: Stiffness Analysis Results for K1

2.2.8 K2, Crankshaft, Second Web to Third Web

K2 was estimated using the Creo 3 Analysis tools. The results are shown in Figure 9. Using Equation 1 and a radius of 49.5 mm, this result suggests a stiffness of 98645 Nm/rad.

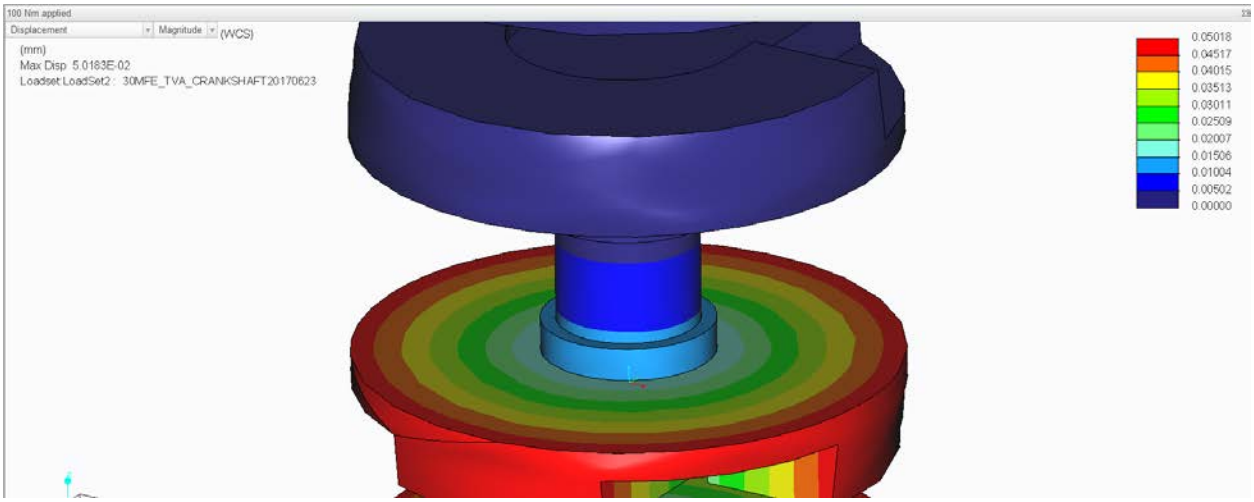

Figure 9: Stiffness Analysis Results for K2

2.2.9 K3, Crankshaft, Fourth Web to End

K3 was estimated using the Creo 3 Analysis tools. The results are shown in Figure 10. Using Equation 1 and a radius of 49.5 mm, this result suggests a stiffness of 86736 Nm/rad.

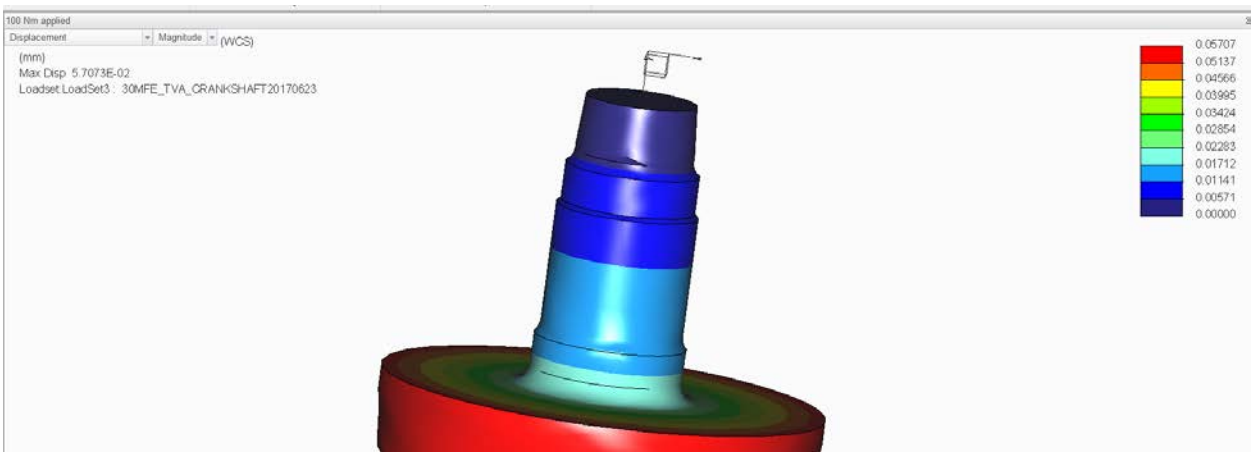

Figure 10: Stiffness Analysis Results for K3

2.2.10 K4, Power Head to Lower Unit

K4 was approximated as only the downshaft and was estimated using the Creo 3 Analysis tools. The results are shown in Figure 11. Using Equation 1 and a radius of 15.85 mm, this result suggests a stiffness of 1373 Nm/rad.

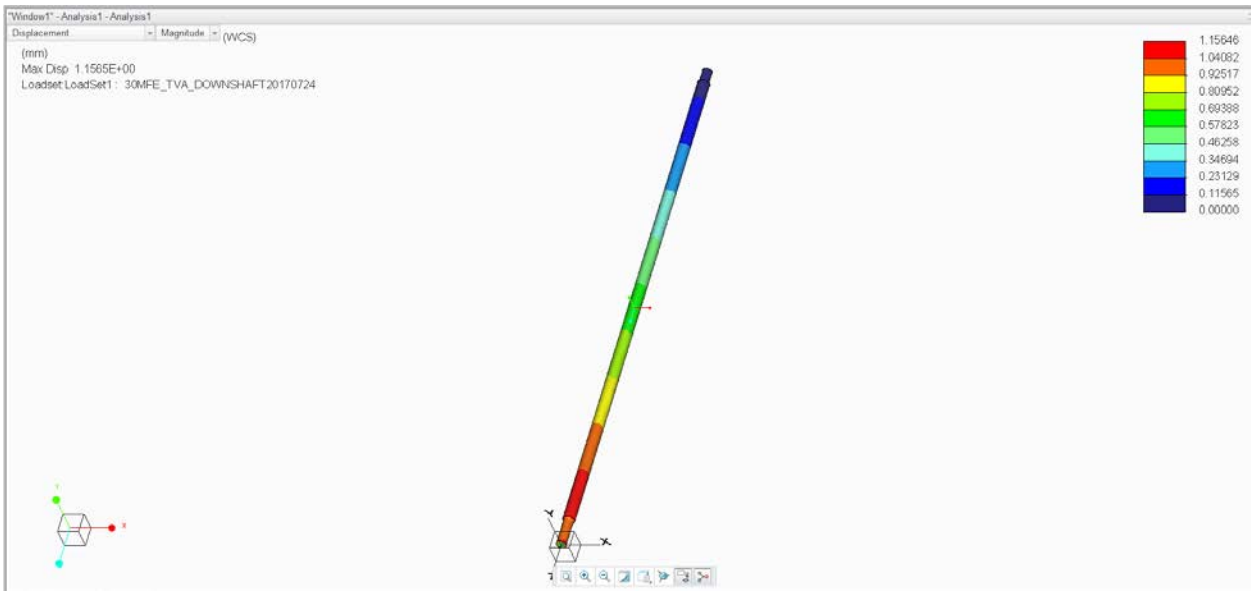

Figure 11: Stiffness Analysis Results for K4

2.2.11 K5, Propshaft and Dyno Drive

K5 is actually an equivalent torsional spring comprised of the propshaft, dyno driveshaft and dyno coupler. The stiffness of the propshaft was estimated using the Creo 3 Analysis tools. The results are shown in Figure 12. Using Equation 1 and a radius of 18.9mm, this result suggests a stiffness of 18986 Nm/rad.

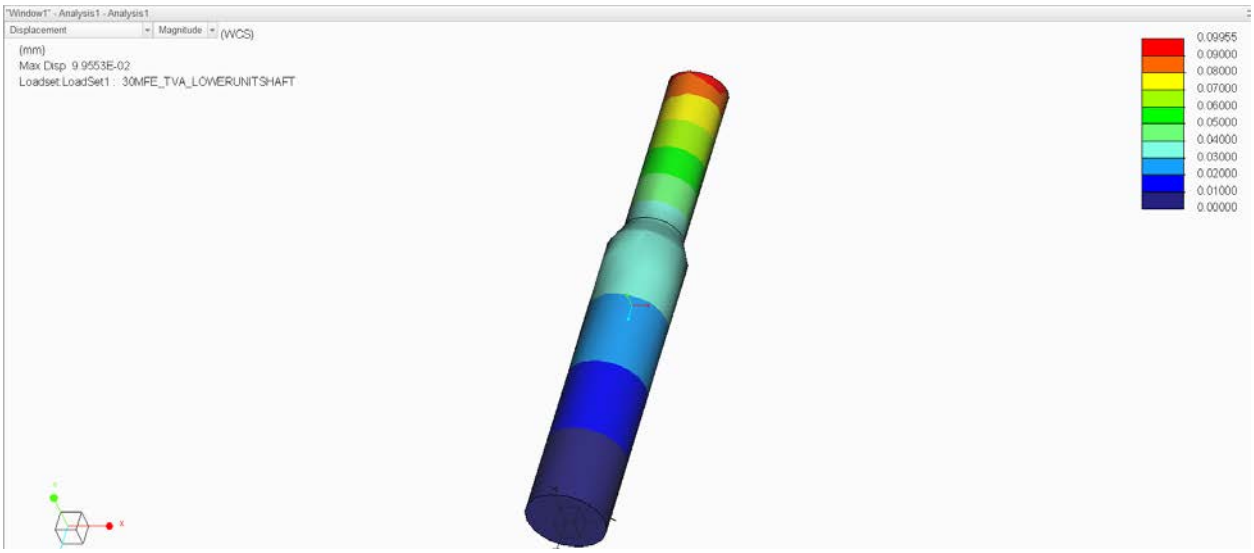

Figure 12: Stiffness Analysis for the Propshaft, part of K5

The next component in the equivalent torsional spring is the dyno driveshaft. Since this component has not been designed yet, the torsional stiffness was estimated to be equivalent to the propshaft at 18986 Nm/rad.

The final component stiffness to consider was the rubber coupling connecting the driveshaft to the dynamometer. This Mercury 76850A2 coupling was acquired by MTU and loaded using a torque wrench and an angle indicator to collect torque and angle measurements. These values and a linear best fit can be found in Figure 13. Rubber couplings have non-linear stiffness and this approximation is not perfect; it was only meant as a first approximation.

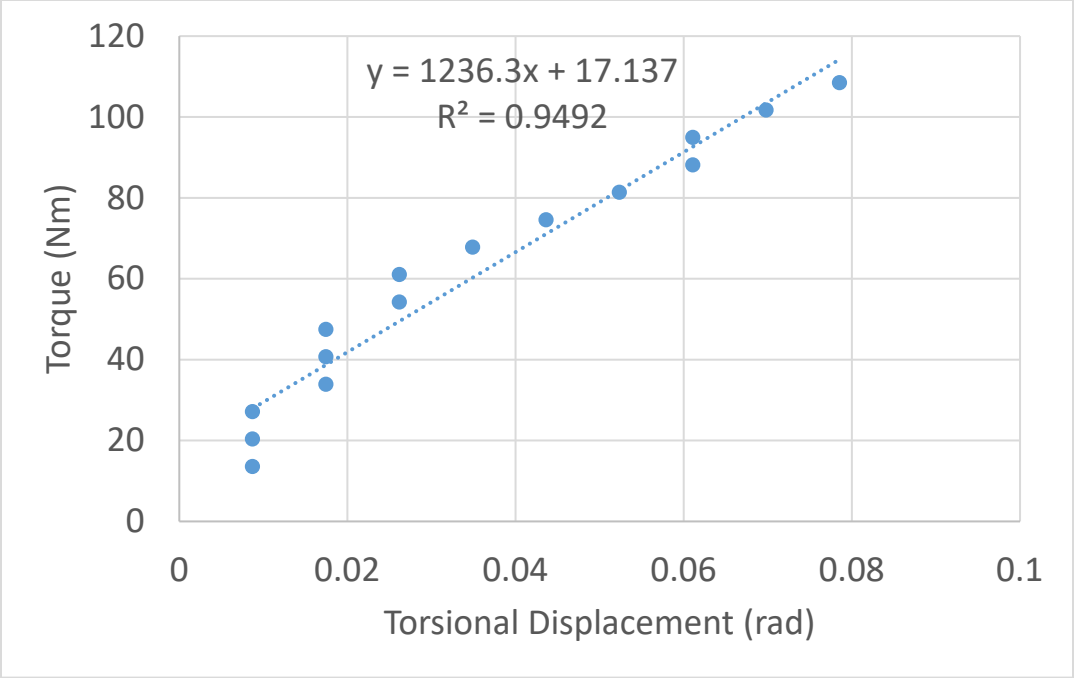

Figure 13: Experimental Results for Stiffness of Mercury Coupler, PN 76850A2

Having estimated the three stiffnesses, an equivalent stiffness was calculated using Equation 7 for a final stiffness of 1094 Nm/rad.

Equation 5: Stiffness of Springs in Series

$$K_{eq} = \frac{1}{\frac{1}{K_1} + \frac{1}{K_2} + \frac{1}{K_3} + \cdots}$$

$Where$:

$K_{eq} = Equivalent\ stiffness$

$K_n = Individual\ segment\ stiffnesses$

2.2.12 Equivalence Calculations and Final Model Values

For a lumped inertia model that includes a speed change through gears, belts, etc. the inertia and stiffnesses values must be corrected for energy differences. This is done by "reflecting" the inertia or stiffness value back to a common shaft in the model using two equations, Equation 5 and Equation 6 for inertia and stiffness, respectively. These equations were taken from A Handbook on Torsional Vibration, by E.J. Nestorides and published in 1958 by Cambridge Press. There derivations can be found there.

Equation 6: Equivalent Inertia

$$J'_A = J_A * \left(\frac{N_a}{N_b}\right)^2$$

$Where$:

$J'_A = Equivalent\ inertia\ of\ component\ A\ as\ seen\ at\ component\ B$

$J_A = True\ inertia\ of\ component\ A$
$\frac{N_a}{N_b} = Speed\ ratio\ of\ component\ B\ to\ component\ A$

Equation 7: Equivalent Torsional Stiffness

$$K_A' = K_A * \left(\frac{N_a}{N_b}\right)^2$$

$Where$:
$K_A' = Equivalent\ stiffness\ of\ between\ component\ A\ and\ component\ B\ as\ seen\ at\ B$
$K_A = True\ stiffness\ of\ component\ A\ to\ component\ B\ connection$
$\frac{N_a}{N_b} = Speed\ ratio\ of\ component\ B\ to\ component\ A$

For this analysis, inertias J5 and J6 with stiffnesses K5 were reflected back to the engine crankshaft. This was an arbitrary selection; the opposite selections could have been made. The speed ratio of the lower unit was 2.15:1 with the propeller speed being 1/ 2.15 that of the engine speed. Equation 5 and Equation 6 were applied in Table 1 and Table 2. These tables show the final values used for the TVA. They also show the values of individual inertias and stiffnesses under the headings "Value 1," "Value 2…" that were added and corrected as appropriate to make the "Equivalent Value." Also, note that for the lower unit that the ½ of the downshaft and the pinion gear were not corrected using Equation 5 as they are ahead of the speed reduction.

Table 1: Inertia Collection and Correction
Values in Orange are Educated Approximations

Inertia Table								
Locator	Description	Value 1	Value 2	Value 3	Value 4	Ratio	Eq. Value	Units
J1	Flywheel	33650.5	0.0	0.0	0.0	1.00	33650.5	kg-mm^2
J2	Upper Cylinder Equivalent Rotating Mass	2246.1	1094.8	0.0	0.0	1.00	3340.8	kg-mm^2
J3	Lower Cylinder Equivalent Rotating Mass	2226.5	1094.8	0.0	0.0	1.00	3321.3	kg-mm^2
J4	Crank End + 1/2 Driveshaft	47.7	16.8	0.0	0.0	1.00	64.5	kg-mm^2
J5	Lower Unit Pinion + Lower Unit Gear + 1/2 Driveshaft + 1/2 Dyno Drive	136.5	293.4	16.8	20.0	0.47	221.0	kg-mm^2
J6	Dyno + 1/2 Dyno Drive	31000.0	20.0	1000.0	0.0	0.47	6927.0	kg-mm^2

Table 2: Stiffness Collection and Correction
Values in Orange are Educated Approximations

Stiffness Table							
Locator	Description	Value 1	Value 2	Value 3	Ratio	Eq. Value	Units
K1	Crankshaft, Flywheel to First Web	185185.2	0.0	0.0	1	185185	Nm/rad
K2	Crankshaft, Second Web to Third Web	98644.9	0.0	0.0	1	98645	Nm/rad
K3	Crankshaft, Fourth Web to End	86735.6	0.0	0.0	1	86736	Nm/rad
K4	Power Head to Lower Unit	1373.0	0.0	0.0	1	1373	Nm/rad
K5	Equivalent Propshaft/Dyno Drive	1236.0	18985.6	18985.6	0.47	237	Nm/rad

2.3 Assumptions and Modeling

The following assumptions were made in producing this torsional vibration model:

- All torque transferring interfaces, including splines, gears, and keyways, were assumed to be infinitely rigid.
- There is no damping, viscous or Coulomb, present in the system.
- The stiffness of the rubber coupling is constant with respect to torque applied.
- The reciprocating mass in each cylinder can be approximated as a constant inertia.
- The rotating mass of the connecting rod “big end” and bearing can be eliminated without significant effect on the results.

The modeling process involved using the Mechanical Library from Siemens LMS Imagine.Lab AMESim to build the model as outlined in Section 2.1. To confirm the equivalent inertia/stiffness calculation methods presented in Section 2.2 a speed reduction version of the model with true inertia and stiffness values was also created. The models produced nearly identical results and are both shown in Figure 12 below.

Figure 14: Siemens LMS Imagine.Lab AMESim Torsional Vibration Models. Left, Equivalent Value Method. Right, AMESim Calculated Method.

3. Torsional Vibration Analysis and Results

To complete the torsional Vibration Analysis, the values collected were assigned to the individual submodels in the AMESim simulation. From there, mode shapes and frequency response functions were computed.

3.1 Mode Shapes

The 5 mode shapes identified by the linear analysis are shown in the subsequent figures. These modes are shown with relative amplitudes in the upper plot and a time history of normalized, forced oscillation in the lower plot. The numbers for each curve/bar correlate to the inertia identifying numbers shown in Figure 1. For visualization purposes, the upper plot can be viewed as positive values twisting clockwise and negative values twisting counter-clockwise. If two adjacent bars have alternate sign, the magnitude of dynamic torque between them is non-zero, which increases stress and accumulated damage.

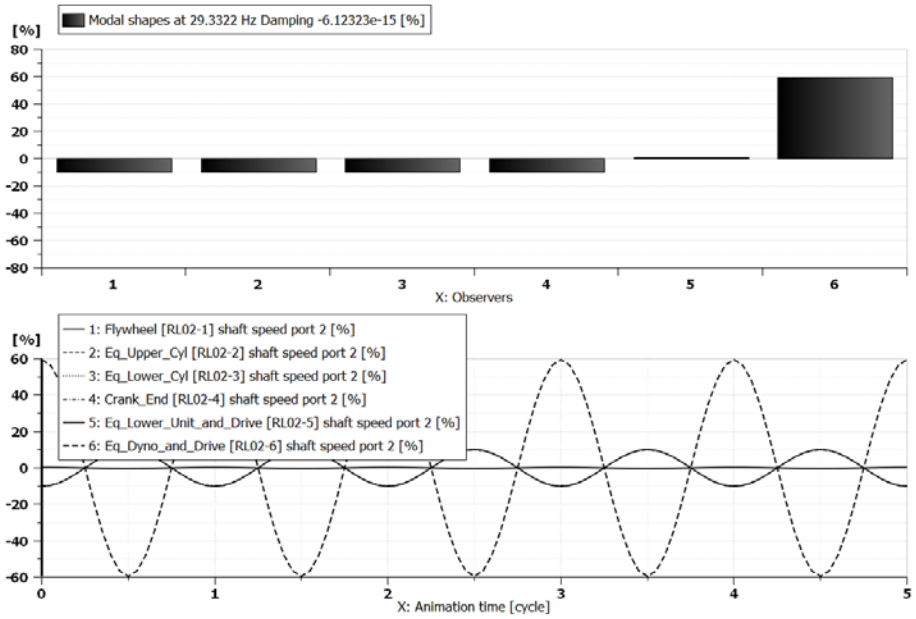

Figure 15: Mode 1, 29 Hz, Engine to Dyno Out of Phase

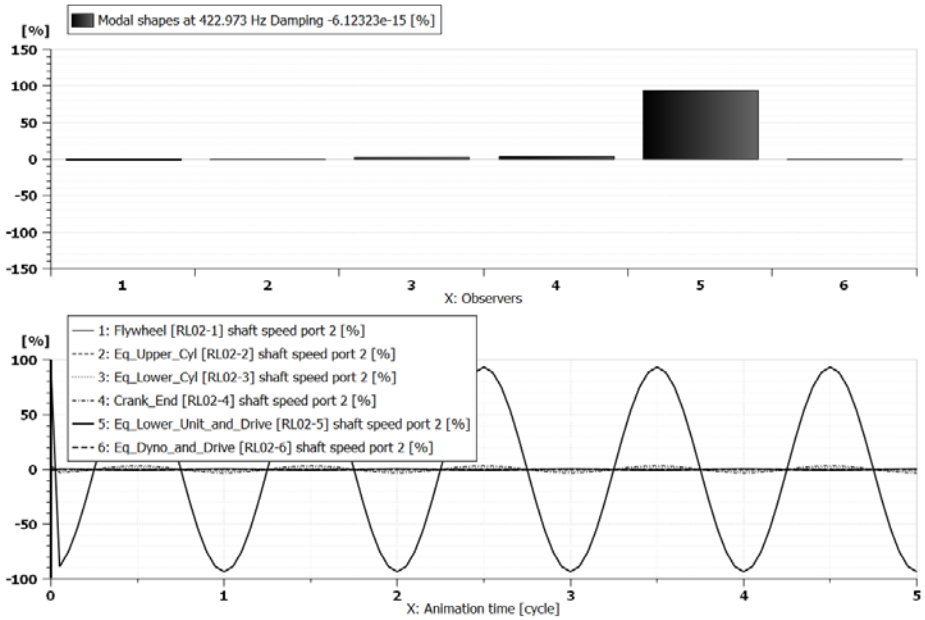

Figure 16: Mode 2, 422 Hz, Lower Unit Oscillation

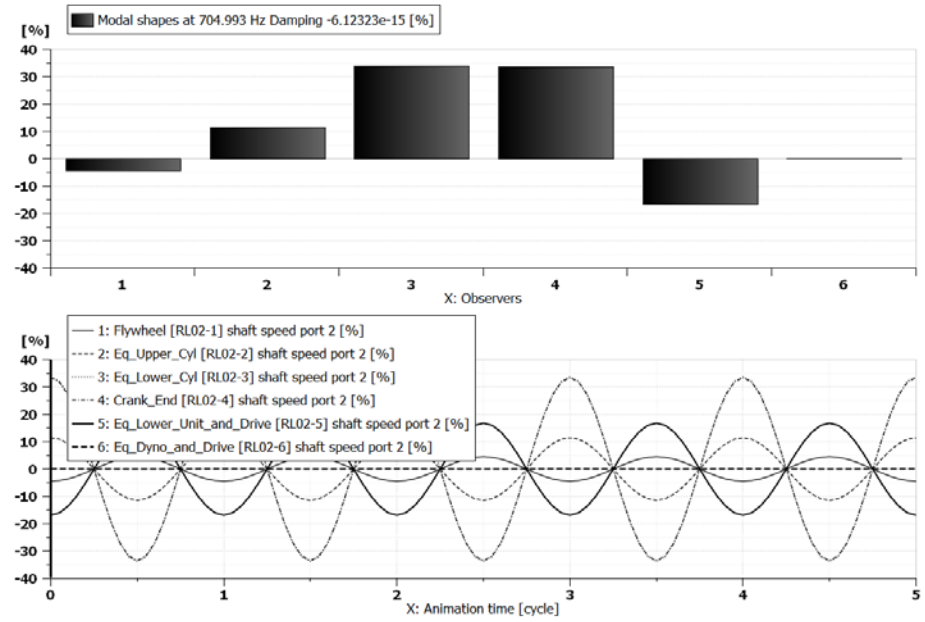

Figure 17: Mode 3, 705 Hz, First Crankshaft Twist Mode

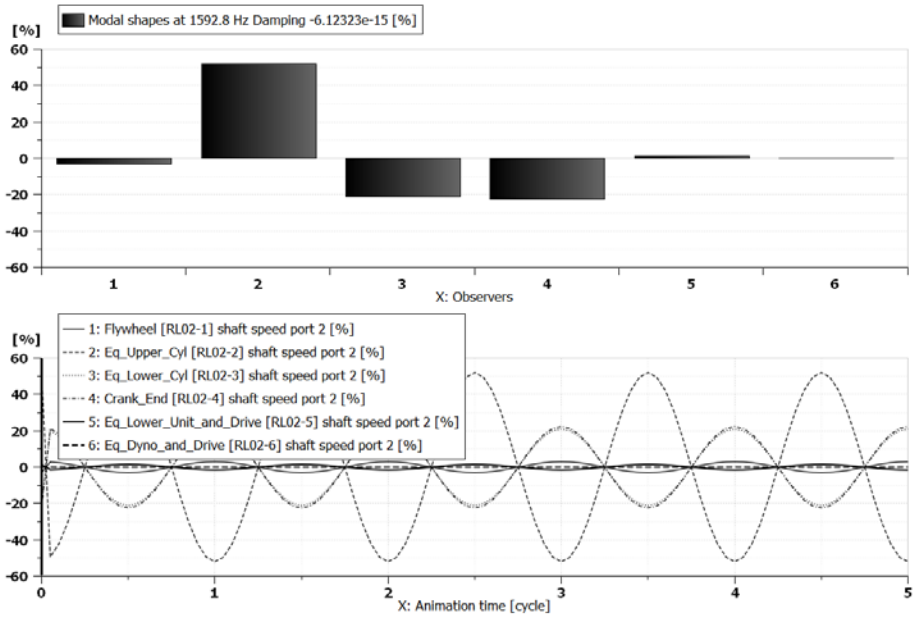

Figure 18: Mode 4, 1592 Hz, Second Crankshaft Twist Mode

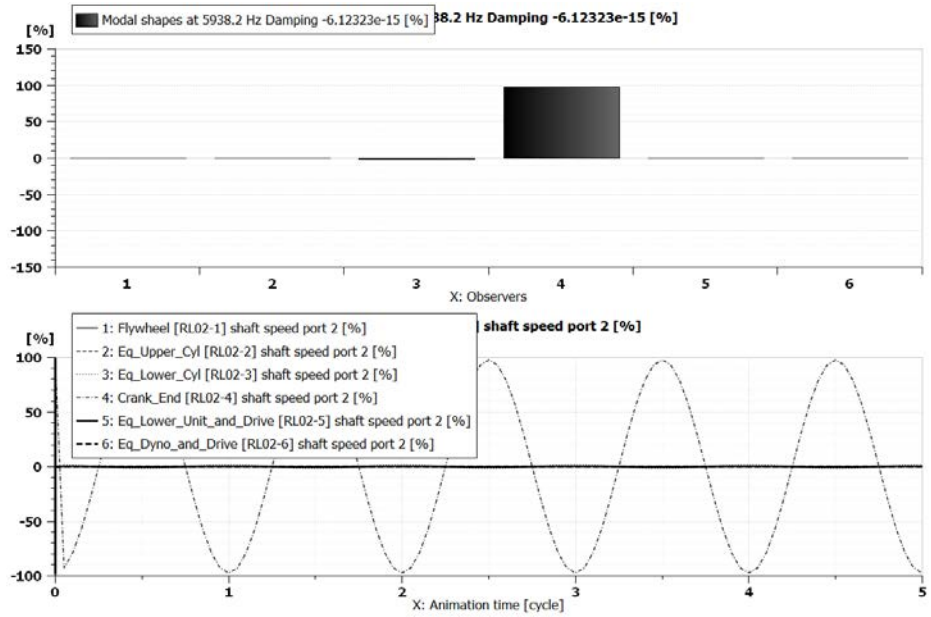

Figure 19: Mode 5, 5938 Hz, End of Crankshaft "Ring"

3.2 Frequency Response Function and Sensitivity

LMS AMESim was used to generate the frequency response function of the inertias' angular speed change to the torque in the "downshaft." This is an approximate function as this analysis did not include damping. What is shown generally is that the previously identified resonance could potentially have damaging effects over a frequency range of approximately 21-35 Hz.

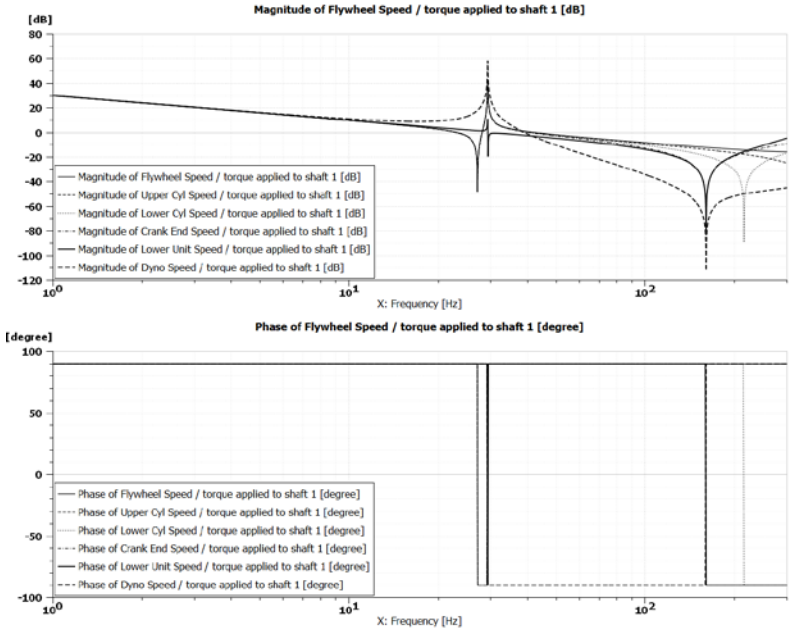

Figure 20: Frequency Response Function of Inertias' Speed Response relative to End of Crankshaft Torque

To determine the sensitivity of this result, the inertia and stiffnesses was varied within unreported analysis runs. This analytical experimentation showed that the main driver of this resonance, as could be expected, was the dynamometer inertia; no other modifiable components altered this behavior as significantly. This result is shown in Figure 21, where they dynamometer inertia was increased by a 2 times and the resulting "resonance window" was shifted from 21-35 Hz to 18-25 Hz. This is a shift in engine operating speed that excites this resonance from 630-1050 to 540-750 RPM.

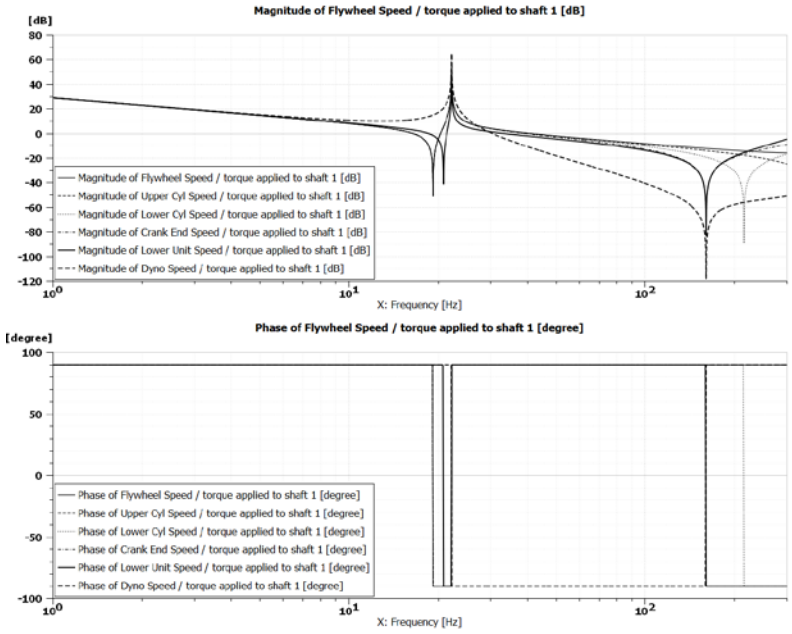

Figure 21: Frequency Response Function of Inertias' Speed Response relative to End of Crankshaft Torque, WITH 2x Equivalent Dyno Inertia

4. Conclusion and Recommendations

An Evinrude 30 MFE engine was disassembled and a torsional vibration model was made using a series of assumptions. This included grouping inertias, estimating torsional stiffnesses, and approximating the anticipated dynamometer connections. Using this information, a torsional vibration analysis was completed using LMS Imagine.Lab AMESim, which in this case was limited to the linearized eigenvalue solution. The result show a torsional resonance in the operating range characterized as the engine flywheel and dynamometer “fighting” each other (oscillating out of phase). This correlates to industry experience of lower unit failures with the anticipated failure mode being overloading the bevel gear set in the lower unit.

Moving forward, the recommendation is to increase the inertia of the low-inertia eddy current dynamometer to 0.057 kg-m^2 or greater such that the amplification of the test-setup-induced resonance is limited to a non-typical engine operating range. Furthermore, it is recommended that this analysis is revisited twice. First, once the final test setup is complete the assumptions made on driveshaft design and dynamometer inertia should be validated. Second, if any in-line torque or high frequency speed measurements are made, this model should be validated for both resonant frequencies and torque/speed fluctuation amplitude.